animals

MDPI

Article

Chicken MHC-B-Linked TRIM27.2 Restricts ALV-J Replication and Modulates Interferon-Related Antiviral Signaling Through Its Interaction with USP19

Shihao Chen [1,*], Qingqing Cai [1], Qiangzhou Wang [1], Na Yin [1], Jiaxing Wang [2], Yulin Bi [1,*] and Guobin Chang [1]

[1] College of Animal Science and Technology, Yangzhou University, Yangzhou 225009, China; mx120250904@stu.yzu.edu.cn (Q.C.); dx120260222@stu.yzu.edu.cn (Q.W.); y15861092032@163.com (N.Y.); gbchang1975@yzu.edu.cn (G.C.)
[2] College of Veterinary Medicine, Yangzhou University, Yangzhou 225009, China; dx120230207@stu.yzu.edu.cn
* Correspondence: mrrchen@yzu.edu.cn (S.C.); ylbi@yzu.edu.cn (Y.B.)

Simple Summary

Avian leukosis virus subgroup J is an important cause of disease and economic losses in poultry. A region of the chicken genome is closely linked to disease resistance, but how genes within this region protect chickens against viral infections remains unclear. In this study, we investigated the antiviral role of a protein produced by one of these genes. We found that this protein reduced viral replication in chicken cells and strengthened their natural antiviral responses. It also interacted with another cellular protein, increased its modification associated with protein breakdown, and reduced its abundance. Reducing the amount of this second protein further suppressed viral replication and enhanced antiviral defenses. These findings reveal a previously unrecognized antiviral function of a gene linked to chicken disease resistance and identify a cellular interaction involved in controlling viral infection. This work provides a basis for further studies aimed at improving disease resistance and reducing the impact of viral diseases on poultry production.

Abstract

Avian leukosis virus subgroup J (ALV-J) causes tumors and immunosuppression in chickens. However, the host factors involved in resistance to ALV-J remain poorly understood. We first examined the transcriptional responses of seven TRIM genes located in the chicken MHC-B region following ALV-J infection. Several TRIM genes showed time-dependent changes, and TRIM27.2 was selected for further study because of its clear response to infection and unknown antiviral function. Overexpression of TRIM27.2 significantly reduced ALV-J RNA levels, viral titers, and Env protein expression in HD11 cells. Transcriptome analysis showed that TRIM27.2 increased the expression of antiviral genes, including MDA5, OASL, MX1, STAT1, and SAMD9L. It also enhanced TBK1- and IRF7-induced IFN-β promoter activity. Deletion of the RING domain markedly reduced the effects of TRIM27.2 on MDA5 and IFN-β expression. Immunoprecipitation followed by mass spectrometry identified USP19 as a TRIM27.2-interacting protein, and their association was supported by co-immunoprecipitation and cytoplasmic colocalization. TRIM27.2 increased the K48-linked ubiquitination of USP19 and reduced its protein level, whereas the proteasome inhibitor MG132 partially restored USP19 expression. Furthermore, USP19 knockdown inhibited ALV-J replication and enhanced TRIM27.2-induced MDA5–IFN-β signaling. These findings show that chicken TRIM27.2 overexpression restricts ALV-J replication in HD11 cells and support a proposed association between USP19 regulation and enhanced interferon-related antiviral responses; the endogenous function and causal pathway remain to be established.

Check for updates

Academic Editor: Peirong Jiao

Received: 29 September 2026
Revised: 25 November 2026
Accepted: 25 November 2026
Published: 27 November 2026

Copyright: © 2026 by the authors. Licensee MDPI, Basel, Switzerland. This article is an open access article distributed under the terms and conditions of the Creative Commons Attribution (CC BY) license.

Keywords: avian leukosis virus subgroup J; TRIM27.2; USP19; proteasomal degradation; innate immunity

1. Introduction

Avian leukosis virus subgroup J (ALV-J) is an oncogenic alpharetrovirus that causes myeloid leukosis, hemangiomas, and other neoplastic diseases in chickens. ALV-J infection can also result in immunosuppression, growth retardation, and reduced production performance [1–4]. No commercial vaccine or specific antiviral drug is currently available for the effective prevention or treatment of ALV-J infection. The virus can establish persistent infection and modulate host innate immune responses [5]. Identifying host factors that restrict ALV-J replication and defining their mechanisms may therefore provide a basis for disease control and the genetic improvement of disease resistance in chickens.

The chicken major histocompatibility complex (MHC) is located in the B locus on microchromosome 16 and is closely associated with immune responses and resistance to infectious diseases [4,5]. In addition to classical MHC genes, the extended MHC-B region contains several tripartite motif-containing (TRIM) genes [6,7]. Typical TRIM proteins contain RING, B-box, and coiled-coil domains and frequently possess a C-terminal PRY/SPRY or B30.2 domain [8]. The RING domain commonly confers E3 ubiquitin ligase activity, whereas the PRY/SPRY domain participates in substrate recognition and protein interactions. TRIM proteins can restrict viral infection by targeting viral components or regulating innate immune signaling [9]. However, the functions of most MHC-B-linked TRIM proteins in chickens remain unknown.

Chickens lack functional retinoic acid-inducible gene I (RIG-I) and mainly depend on melanoma differentiation-associated protein 5 (MDA5) to recognize cytoplasmic viral RNA and induce interferon beta (IFN-β) and interferon-stimulated genes [10,11]. Chicken TRIM25 enhances the MDA5-mediated type I interferon response and inhibits avian leukosis virus subgroup A replication [12], whereas ALV-J infection can alter MDA5-related antiviral signaling [13,14]. These findings indicate that chicken TRIM proteins can regulate MDA5-related immune responses and that MDA5 signaling is involved in ALV-J infection, supporting further investigation of whether MHC-B-linked TRIM proteins affect ALV-J replication through MDA5-related signaling.

Mammalian TRIM27 is a RING-type E3 ubiquitin ligase that promotes K48-linked ubiquitination and proteasomal degradation of TANK-binding kinase 1 (TBK1), thereby suppressing type I interferon production. The deubiquitinating enzyme USP7 enhances this activity by stabilizing TRIM27 [15,16]. In contrast, duck TRIM27-L enhances MAVS signaling and antiviral gene expression, although this protein is absent in chickens and turkeys [17]. TRIM27-related proteins may therefore have different functions among species. Ubiquitin-specific protease 19 (USP19) is a deubiquitinating enzyme that regulates autophagy and type I interferon responses by modifying the ubiquitination of Beclin-1, TRAF3, and MAVS [18–20]. However, the immune functions of chicken TRIM27.2 and USP19 and the relationship between these proteins remain unclear.

In this study, we first examined the expression of seven TRIM genes in the chicken MHC-B region following ALV-J infection and selected TRIM27.2 for further analysis based on its clear time-dependent response. The effect of TRIM27.2 on ALV-J replication was evaluated by measuring viral RNA, infectious viral titers, and Env protein expression. Transcriptome sequencing and domain-deletion analysis were used to examine its regulation of MDA5–IFN-β-related antiviral signaling. Immunoprecipitation–mass spectrometry, co-immunoprecipitation, immunofluorescence, ubiquitination analysis, and siRNA-mediated

knockdown were subsequently used to investigate the interaction between TRIM27.2 and USP19 and its role in the antiviral response to ALV-J.

2. Materials and Methods

2.1. Cells, Virus, and Reagents

The chicken macrophage-like cell line HD11 and chicken embryo fibroblast cell line DF-1 were maintained in our laboratory. Both cell lines were cultured in Dulbecco's modified Eagle medium (DMEM; Gibco, Grand Island, NY, USA) supplemented with 10% fetal bovine serum (FBS; Gibco) and 1% penicillin–streptomycin at 37 °C in a humidified atmosphere containing 5% CO_2. The ALV-J GY3 strain was kindly provided by Professor Aijian Qin of Yangzhou University and was subsequently propagated and maintained in our laboratory. The virus was amplified in DF-1 cells, and infectious viral titers were determined using the 50% tissue culture infectious dose ($TCID_{50}$) assay.

2.2. ALV-J Infection

To examine the expression patterns of TRIM genes in the chicken MHC-B region following ALV-J infection, HD11 cells were infected with the ALV-J GY3 strain at a multiplicity of infection of 1. Cells were collected at 0, 12, 24, 36, and 48 h post-infection for total RNA extraction and qRT-PCR analysis. Mock-infected cells were treated with an equal volume of virus-free culture medium. For viral infection, cells were incubated with the viral inoculum for 1 h at 37 °C. The inoculum was then removed, and the cells were washed three times with phosphate-buffered saline (PBS). Fresh DMEM containing 2% FBS was subsequently added, and the cells or culture supernatants were collected at the indicated time points for further analysis.

2.3. Construction of Recombinant Plasmids and TRIM27.2 Deletion Mutants

Gene-specific primers were designed using the chicken TRIM27.2 RefSeq transcript (NM_001099359.2) and the predicted chicken USP19 transcript variant X7 (XM_015293327.4) as references. The full-length coding sequences of both genes were amplified from cDNA prepared from chicken HD11 cells. The PCR products were purified, digested with restriction enzymes at sites introduced by the primers, and cloned into pCAGGS-N-Myc and pCAGGS-HA to generate pCAGGS-N-Myc-TRIM27.2 and pCAGGS-HA-USP19, respectively. Both constructs were verified by bidirectional Sanger sequencing. The experimentally determined coding sequences were deposited in GenBank under accession numbers QB383493 (TRIM27.2) and QB383494 (USP19) and were used in all subsequent analyses. The predicted USP19 sequence (XM_015293327.4) was used only for primer design. Based on the predicted domain architecture of TRIM27.2, three deletion mutants were constructed: a RING-domain deletion mutant (delR), a double-deletion mutant lacking the B-box and coiled-coil domains (delB&C), and a SPRY-domain deletion mutant (delS). All deletion mutants were cloned into the pCAGGS-N-Myc vector. The recombinant plasmids were verified by Sanger sequencing performed by GENEWIZ Co., Ltd (Suzhou, China). to confirm the inserted sequences, reading frames, and tag junctions. Plasmids were extracted using an endotoxin-free plasmid extraction kit (Tiangen Biotech, Beijing, China), and their concentrations and purity were measured using a Nano-100 microvolume spectrophotometer (Allsheng Instruments, Hangzhou, China).

2.4. Design and Synthesis of siRNAs

Three small interfering RNAs (siRNAs) targeting the coding sequence of chicken USP19 were designed and synthesized and designated siUSP19_1, siUSP19_2, and siUSP19_3. A non-targeting siRNA (siNC) was used as the negative control. All siRNAs were designed

and synthesized by GeneAdv Biotech (Suzhou, China). Their sequences are listed in Table S1.

2.5. Cell Transfection

HD11 cells were seeded in culture plates of the appropriate sizes and transfected when they reached approximately 70–80% confluence. Unless otherwise specified, 1 μg of plasmid DNA per well in 12-well plates or siRNA at a final concentration of 50 nmol/L was used for transfection, as appropriate. Plasmids and siRNAs were transfected using the TransIT-X2 Dynamic Delivery System (Mirus Bio, Madison, WI, USA) according to the manufacturer's instructions. The corresponding empty vectors, pCAGGS-N-Myc or pCAGGS-HA, were used as plasmid controls, and siNC was used as the negative control for siRNA transfection. Unless otherwise stated, cells were cultured for 24 or 48 h after transfection and then collected for qRT-PCR, Western blotting, dual-luciferase reporter assays, co-immunoprecipitation, immunofluorescence, or ubiquitination analysis.

2.6. RNA Extraction, Reverse Transcription, and qRT-PCR

Total RNA was extracted from cells using TRIzol reagent (Invitrogen, Carlsbad, CA, USA) according to the manufacturer's instructions. RNA concentration and purity were measured using a Nano-100 microvolume spectrophotometer (Allsheng Instruments, Hangzhou, China). Equal amounts of total RNA were reverse-transcribed into cDNA using HiScript III RT SuperMix (Vazyme, Nanjing, China). qRT-PCR was performed using AceQ qPCR SYBR Green Master Mix (Vazyme, Nanjing, China) on a CFX Connect Real-Time PCR Detection System (Bio-Rad, CA, USA). The reaction mixture and amplification conditions were set according to the manufacturer's instructions. Each sample was analyzed in three technical replicates. Chicken β-actin was used as the reference gene, and relative gene expression was calculated using the $2^{-\Delta\Delta Ct}$ method. The primer sequences are listed in Table S2.

2.7. Western Blot Analysis

Cells were washed with ice-cold PBS and lysed on ice in RIPA buffer containing a protease inhibitor cocktail (Beyotime Biotechnology, Shanghai, China). Cell lysates were centrifuged at 12,000× *g* for 10 min at 4 °C, and the supernatants were collected. Total protein concentrations were measured using a bicinchoninic acid assay kit (Beyotime). Equal amounts of protein were mixed with SDS-PAGE loading buffer and heated at 100 °C for 10 min. Proteins were separated by SDS-PAGE and transferred onto 0.45 μm nitrocellulose membranes (Millipore, MA, USA).

The membranes were blocked with 5% non-fat milk in Tris-buffered saline containing Tween 20 for 2 h at room temperature and then incubated with the appropriate primary antibodies overnight at 4 °C. The primary antibodies included anti-Myc (1:1000; MBL, Tokyo, Japan, M192-3), anti-HA (1:1000; Cell Signaling Technology, Danvers, MA, USA, #3724), anti-β-actin (1:3000; ABclonal, Wuhan, China, AC026), anti-GAPDH (1:3000; ABclonal, Wuhan, China, AC033), anti-α-tubulin (1:3000; MBL, Tokyo, Japan, PM054), and a laboratory-produced anti-ALV-J Env antibody (1:1000). After washing with TBST, the membranes were incubated with horseradish peroxidase-conjugated goat anti-rabbit or goat anti-mouse IgG secondary antibodies (1:5000; Abcam, Cambridge, UK) for 1 h at room temperature. Protein signals were detected using an enhanced chemiluminescence substrate (Thermo Fisher Scientific, Waltham, MA, USA) and captured using a FluorChem Q imaging system (ProteinSimple, San Jose, CA, USA). Band intensities were measured using ImageJ software (version 1.54p, Bethesda, MD, USA). Target protein signals were normalized to β-actin, GAPDH, or α-tubulin, as appropriate, and are presented relative to the corresponding control group.

2.8. Viral Titer Determination

Cell culture supernatants were collected from each treatment group, filtered through a 0.22 μm membrane, with 10-fold serial dilutions. The diluted samples were inoculated onto confluent DF-1 cell monolayers in 96-well plates, with eight replicate wells for each dilution. After incubation at 37 °C for 6 days, virus-positive wells were identified by immunofluorescence staining using the anti-ALV-J Env antibody. The 50% tissue culture infectious dose was calculated using the Reed–Muench method, and viral titers are expressed as log $_{10}$TCID$_{50}$/mL.

2.9. Transcriptome Sequencing and Bioinformatic Analysis

HD11 cells were divided into an empty-vector control group transfected with pCAGGS-N-Myc and a TRIM27.2 overexpression group transfected with pCAGGS-N-Myc-TRIM27.2. Three independent biological replicates were included in each group. At 24 h after transfection, total RNA was extracted using TRIzol reagent. RNA concentration and purity were measured using a Nano-100 microvolume spectrophotometer, and RNA integrity was assessed using an Agilent 2100 Bioanalyzer (Agilent Technologies, Santa Clara, CA, USA). RNA samples that met the quality requirements were submitted to Gene Denovo Biotechnology Co., Ltd. (Guangzhou, China) for mRNA library construction and transcriptome sequencing. After adapter removal and low-quality read filtering, the resulting high-quality clean reads were aligned to the chicken reference genome GRCg6b. HISAT2 was used for read alignment, featureCounts was used for gene-level read counting, and DESeq2 was used for differential expression analysis. Differentially expressed genes were identified using thresholds of false discovery rate < 0.05 and $|\log_2$ fold change$| \geq 1$. Principal component analysis was used to evaluate overall gene expression patterns and reproducibility among biological replicates. Gene Ontology and Kyoto Encyclopedia of Genes and Genomes analyses were performed for functional annotation and enrichment analysis of the differentially expressed genes. Terms with an adjusted p value or FDR < 0.05 were considered significantly enriched.

2.10. Immunoprecipitation–Mass Spectrometry Analysis

HD11 cells were transfected with pCAGGS-N-Myc-TRIM27.2. Immunoprecipitation was performed using anti-Myc-conjugated magnetic beads, with isotype IgG-conjugated magnetic beads used as a negative control. At 48 h after transfection, the cells were washed with ice-cold PBS and lysed on ice for 40 min using NP-40 immunoprecipitation buffer containing a protease inhibitor cocktail. The lysates were centrifuged at 12,000× g for 15 min at 4 °C to remove cellular debris. A portion of each supernatant was retained as the input. The remaining lysate was incubated with pre-equilibrated anti-Myc-conjugated magnetic beads overnight at 4 °C with gentle rotation. The beads were collected using a magnetic separator, washed five times with ice-cold lysis buffer, and boiled in SDS-PAGE loading buffer to elute the bound proteins. IgG control samples were processed under the same conditions.

The eluted proteins were separated by SDS-PAGE, and the gel was stained with Coomassie Brilliant Blue staining solution (Beyotime). The corresponding gel regions from the TRIM27.2 immunoprecipitation and control groups were excised and submitted to Hangzhou Cosmos Wisdom Biotechnology Co., Ltd (Hangzhou, China). for liquid chromatography–tandem mass spectrometry analysis. The mass spectrometry data were searched against the chicken protein database using MaxQuant (version 2.6.7.0). Proteins also detected in the IgG control samples were considered potential nonspecific binders and excluded from candidate selection. Candidate TRIM27.2-interacting proteins were selected based on the number of unique peptides, sequence coverage, and enrichment

relative to the IgG controls. The proteins identified by LC–MS/MS analysis, together with their identification and abundance information, are listed in Supplementary Table S3.

2.11. Co-Immunoprecipitation Analysis

HD11 cells were cotransfected with pCAGGS-N-Myc-TRIM27.2 and pCAGGS-HA-USP19. The corresponding empty-vector combinations were used as negative controls. At 48 h after transfection, the cells were washed with ice-cold PBS and lysed in immunoprecipitation buffer supplemented with a protease inhibitor cocktail. The lysates were clarified by centrifugation at 4 °C, and a portion of each supernatant was retained as the input. The remaining lysates were incubated with pre-equilibrated anti-Myc-conjugated magnetic beads or IgG-conjugated magnetic beads overnight at 4 °C with gentle rotation. The beads were collected using a magnetic separator, washed five times with ice-cold lysis buffer, and boiled in SDS-PAGE loading buffer to elute the bound proteins. The immunoprecipitated proteins were analyzed by Western blotting with an anti-HA antibody.

2.12. Immunofluorescence and Colocalization Analysis

HD11 cells were seeded in culture plates containing sterile glass coverslips and transfected with pCAGGS-N-Myc-TRIM27.2 alone or cotransfected with pCAGGS-N-Myc-TRIM27.2 and pCAGGS-HA-USP19. At 24 h after transfection, the cells were washed with PBS and fixed with 4% paraformaldehyde for 15 min at room temperature. The cells were then permeabilized with 0.1% Triton X-100 for 10 min and blocked with PBS containing 5% bovine serum albumin for 1 h at room temperature. The cells were incubated with anti-Myc (1:300; MBL, Tokyo, Japan, M192-3) and anti-HA (1:300; Cell Signaling Technology, MA, USA #3724) antibodies overnight at 4 °C. After washing with PBS, the cells were incubated with the corresponding Alexa Fluor 488- or Alexa Fluor 594-conjugated secondary antibodies (1:200; Abconal, Wuhan, China) for 1 h at room temperature in the dark. Cell nuclei were subsequently counterstained with 4′,6-diamidino-2-phenylindole. Images were acquired using a ZEISS LSM 880 laser confocal microscope (Carl Zeiss, Jena, Germany). The same laser power, detector gain, and image acquisition settings were used for all experimental groups. Fluorescence intensity profiles along the selected lines were generated using the microscope software (ZEISS ZEN 3.10).

2.13. Ubiquitination Analysis

To examine the effects of proteasome and lysosome inhibitors on the protein abundance of TRIM27.2 and USP19, HD11 cells were cotransfected with pCAGGS-HA-USP19 and pCAGGS-N-Myc-TRIM27.2. Before collection, the cells were treated for 12 h with dimethyl sulfoxide as the vehicle control, chloroquine at 50 μmol/L, or MG132 at 20 μmol/L. The cells were then collected for Western blot analysis. To determine the type of ubiquitin chains attached to USP19, HD11 cells were cotransfected with pCAGGS-HA-USP19, pCAGGS-N-Myc-TRIM27.2, and His-tagged K48 or K63 ubiquitin expression constructs. Before collection, the cells were treated with MG132 at 20 μmol/L for 6 h. The cells were lysed under denaturing conditions to disrupt non-covalent protein interactions. The denatured lysates were subsequently diluted with immunoprecipitation buffer to conditions compatible with antibody binding. HA-USP19 was immunoprecipitated using the anti-HA antibody, and K48- or K63-linked polyubiquitination of USP19 was detected by Western blotting using an anti-His antibody.

2.14. Dual-Luciferase Reporter Assay

DF-1 cells were seeded in 24-well plates and transfected at approximately 70–80% confluence. Each well was cotransfected with the chicken IFN-β promoter firefly luciferase

reporter plasmid pGL3-IFN-β, the pRL-TK Renilla luciferase control plasmid, pCAGGS-N-Myc-TRIM27.2 or the corresponding empty vector, and either p3.1-TBK1 or p3.1-IRF7. The amounts of plasmid used per well were 100 ng of pGL3-IFN-β, 10 ng of pRL-TK, 200 ng of pCAGGS-N-Myc-TRIM27.2 or empty vector, and 200 ng of p3.1-TBK1 or p3.1-IRF7. At 24 h after transfection, firefly and Renilla luciferase activities were measured sequentially using a dual-luciferase reporter assay kit (Vazyme, Nanjing, China) according to the manufacturer's instructions. Firefly luciferase activity was normalized to Renilla luciferase activity. Relative IFN-β promoter activity was calculated using the corresponding empty-vector group as the reference. Three technical replicates were included for each treatment, and each experiment was independently repeated at least three times.

2.15. Statistical Analysis

Quantitative data are presented as the mean ± standard deviation. Statistical analyses were performed using GraphPad Prism 8.0 (GraphPad Software, San Diego, CA, USA). Comparisons between two groups were performed using a two-tailed unpaired Student's *t*-test. Data involving three or more groups with one independent factor were analyzed using one-way analysis of variance followed by Tukey's or Dunnett's multiple-comparison test, as appropriate. Experiments involving two independent factors were analyzed using two-way analysis of variance followed by the appropriate correction for multiple comparisons. A p value < 0.05 was considered statistically significant. Unless otherwise stated, all experiments were independently repeated at least three times. The sample sizes are specified in the corresponding figure legends.

3. Results

3.1. Expression Patterns of MHC-B-Linked TRIM Genes Following ALV-J Infection

Analysis of the chicken telomere-to-telomere (T2T) genome assembly identified seven TRIM genes in and around the MHC-B region (Figure 1A). To characterize their temporal expression patterns, the relative expression levels of these seven TRIM genes were measured in ALV-J-infected HD11 cells from 0 to 48 h post-infection (Figure 1B–H). TRIM7.1 expression decreased significantly at 24 and 36 h ($p < 0.05$). TRIM7.2 was initially downregulated at 12 h ($p < 0.05$) but subsequently increased, reaching approximately 3.5-fold its baseline level at 48 h ($p < 0.01$). TRIM27.1 expression increased at later time points, reaching approximately 7-fold its baseline level at 48 h ($p < 0.01$). TRIM39.1 was significantly downregulated at 12 h ($p < 0.01$) but subsequently increased to approximately 4-fold its baseline level at 48 h ($p < 0.01$). TRIM41 showed the strongest response, with its expression increasing approximately 33-fold at 48 h ($p < 0.01$). In contrast, TRIM27.2 expression decreased to approximately 0.3-fold its baseline level at 12 h and remained below baseline throughout the observation period. Similarly, TRIM39.2 expression declined markedly, reaching very low levels at 36–48 h. These results revealed distinct temporal expression patterns among the seven TRIM genes. Given its pronounced and sustained downregulation and the limited understanding of its role in ALV-J infection, TRIM27.2 was selected for further functional and mechanistic investigations.

3.2. Expression of TRIM27.2 and Its Effect on ALV-J Replication

To determine the subcellular localization of TRIM27.2, Myc-tagged TRIM27.2 was expressed in HD11 cells and detected by immunofluorescence. Myc-TRIM27.2 fluorescence was detected in both the cytoplasm and nucleus of transfected cells (Figure 2A). To examine the effect of TRIM27.2 on ALV-J replication, HD11 cells overexpressing TRIM27.2 were infected with ALV-J, and viral RNA, infectious viral titers, and viral protein expression were measured. TRIM27.2 overexpression significantly reduced ALV-J RNA levels compared

with the empty-vector control ($p < 0.05$; Figure 2B). The viral titer in the culture supernatant was also significantly lower in the TRIM27.2 overexpression group ($p < 0.05$; Figure 2C). Western blot analysis further showed that TRIM27.2 overexpression significantly reduced ALV-J Env protein expression ($p < 0.01$; Figure 2D). These results indicate that TRIM27.2 inhibits ALV-J replication in HD11 cells.

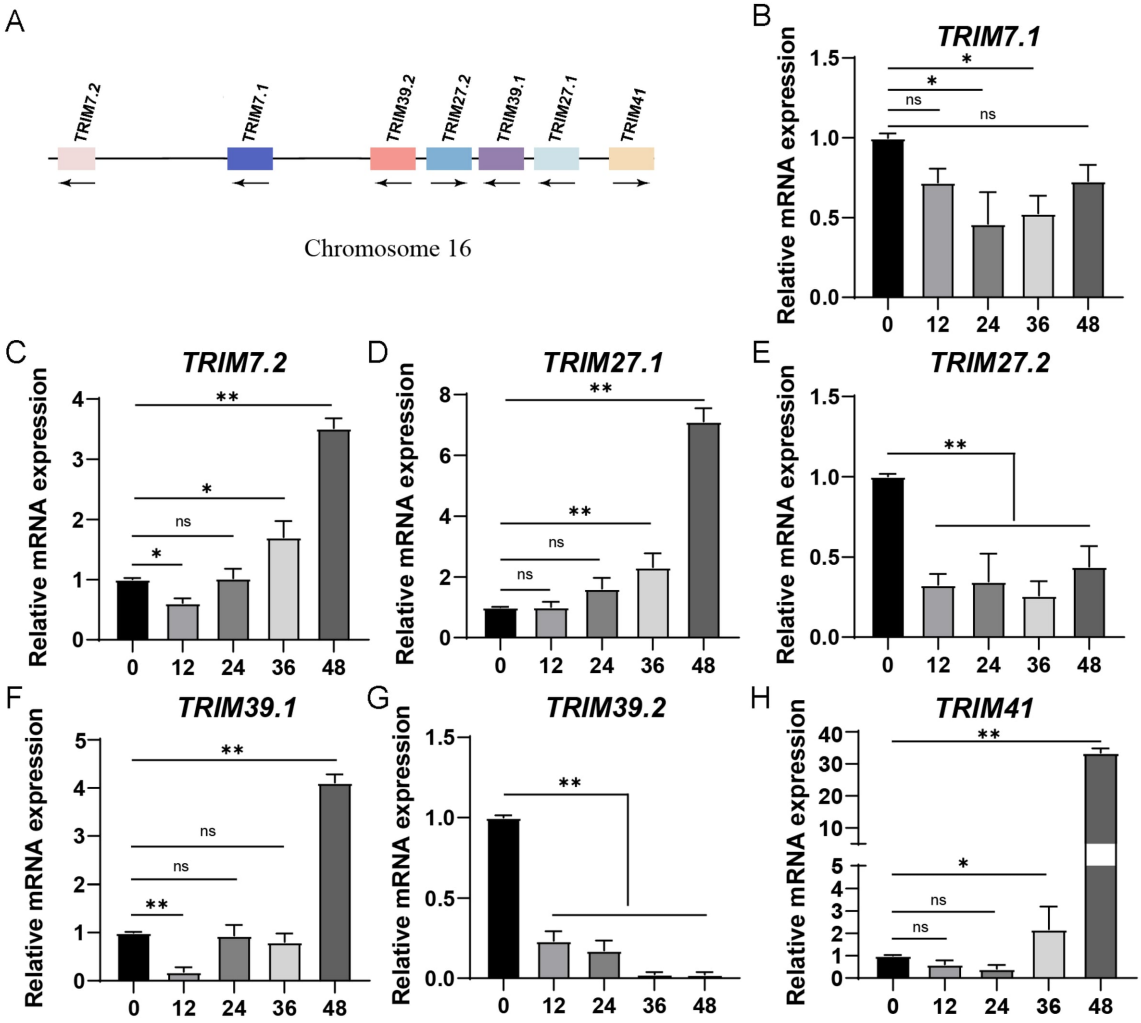


Figure 1. Expression of chicken MHC-B-linked TRIM genes following ALV-J infection. (**A**) Schematic representation of the TRIM gene cluster in the MHC-B region of chicken chromosome 16. Arrows indicate the direction of transcription. (**B**–**H**) Relative mRNA expression levels of TRIM7.1 (**B**), TRIM7.2 (**C**), TRIM27.1 (**D**), TRIM27.2 (**E**), TRIM39.1 (**F**), TRIM39.2 (**G**), and TRIM41 (**H**) in HD11 cells at 0, 12, 24, 36, and 48 h after ALV-J infection. β-Actin was used as the reference gene, and the 0 h infected-group sample was used as the baseline reference for the time-course comparison. A broken y-axis is used in panel (**H**). Data are presented as the mean ± SD ($n = 3$). * $p < 0.05$; ** $p < 0.01$; ns, not significant.

3.3. TRIM27.2 Enhances Antiviral Gene Expression and IFN-β Signaling

To investigate the transcriptional changes associated with the antiviral effect of TRIM27.2, we performed transcriptome sequencing of HD11 cells transfected with a TRIM27.2 expression construct or the empty vector. PCA revealed a clear separation between the CTRL and TRIM27.2-overexpressing groups, with PC1 and PC2 accounting for 97.4% and 1.6% of the total variance, respectively (Supplementary Figure S1 and Table S4). We identified 573 differentially expressed genes (DEGs), of which 378 were upregulated and 195 were downregulated (Figure 3A,B). A heatmap of immune-related genes showed

distinct expression patterns between the two groups. IFIH1 (MDA5), OASL, MX1, STAT1, SAMD9L, IFIT5, CH25H, CMPK2, TLR7, and CCR2 were upregulated following TRIM27.2 overexpression, whereas IL-1β, IL-8L2, NOS2, CCL4, CCL5, CCL20, CCL3, and NFKBIA were downregulated (Figure 3C). Gene Ontology analysis showed enrichment of terms related to the extracellular region, cytokine activity, chemokine activity, cytokine receptor binding, immune responses, leukocyte chemotaxis, inflammation, and defense responses (Figure 3D). Kyoto Encyclopedia of Genes and Genomes analysis identified enrichment of pathways related to cytokine–cytokine receptor interactions, Toll-like receptor signaling, RIG-I-like receptor signaling, NOD-like receptor signaling, cytosolic DNA sensing, C-type lectin receptor signaling, and influenza A (Figure 3E).

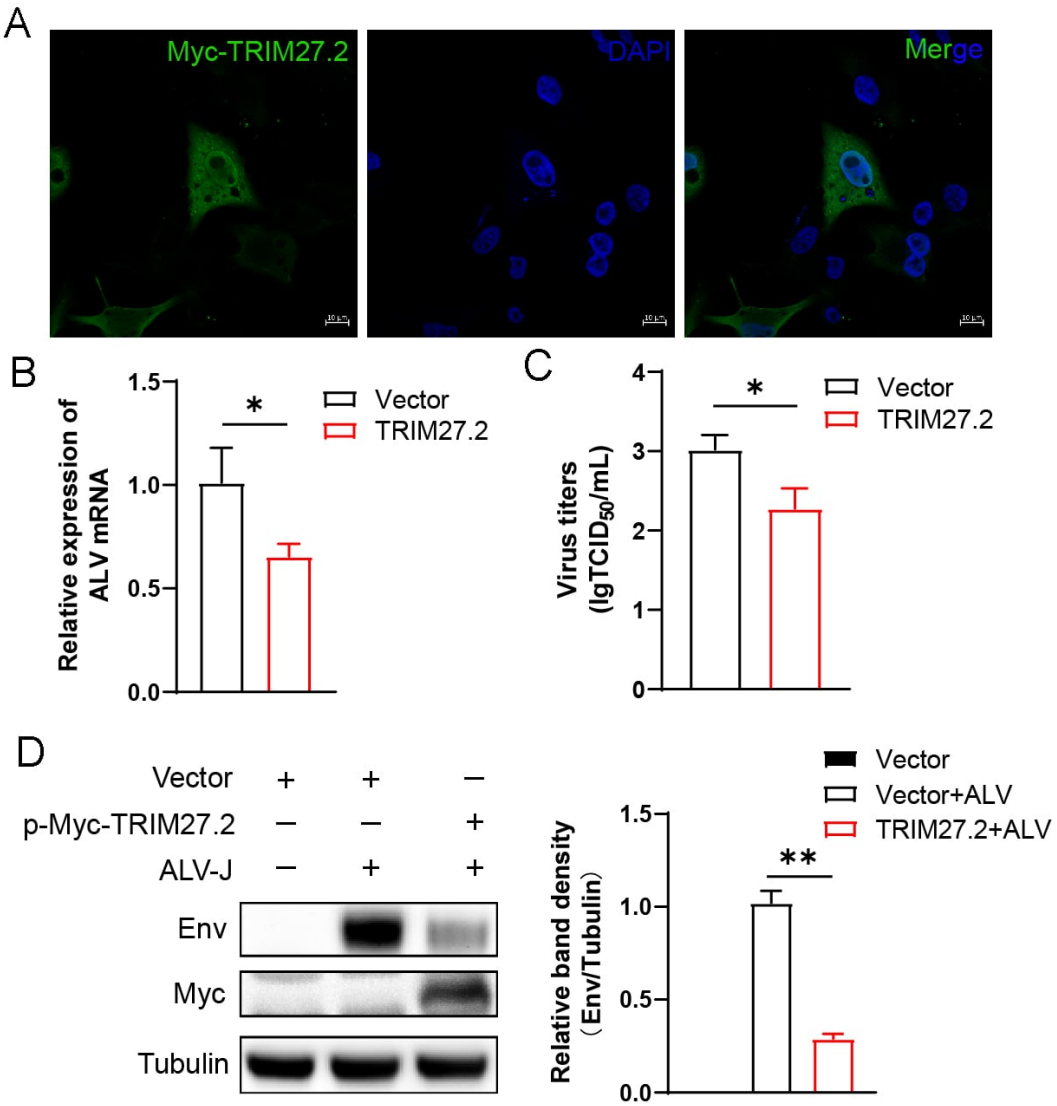


Figure 2. Subcellular localization of TRIM27.2 and its effect on ALV-J replication. (**A**) Immunofluorescence images of HD11 cells expressing Myc-TRIM27.2. Myc-TRIM27.2 is shown in green, and nuclei stained with DAPI are shown in blue. Scale bar = 10 μm. (**B**) Relative ALV-J RNA levels in HD11 cells overexpressing TRIM27.2. (**C**) Viral titers in the culture supernatants of HD11 cells overexpressing TRIM27.2, expressed as $lgTCID_{50}$/mL. (**D**) Western blot analysis of ALV-J Env protein expression following TRIM27.2 overexpression (**left**) and densitometric analysis of the protein bands (**right**). Data are presented as the mean ± SD from three independent biological replicates. * $p < 0.05$; ** $p < 0.01$.

We selected representative genes for qRT-PCR validation. TRIM27.2 overexpression significantly increased the mRNA levels of IFIH1, OASL, MX1, STAT1, and SAMD9L ($p < 0.01$) and decreased those of IL-1β and NOS2 ($p < 0.05$; Figure 3F), consistent with the transcriptome results. We next used a dual-luciferase reporter assay to examine the effect of TRIM27.2 on IFN-β promoter activity. TRIM27.2 significantly enhanced promoter activity in cells expressing TBK1 or IRF7 ($p < 0.01$; Figure 3G). Together, these findings show that TRIM27.2 overexpression alters the expression of immune-related genes and enhances TBK1- or IRF7-induced IFN-β promoter activity.

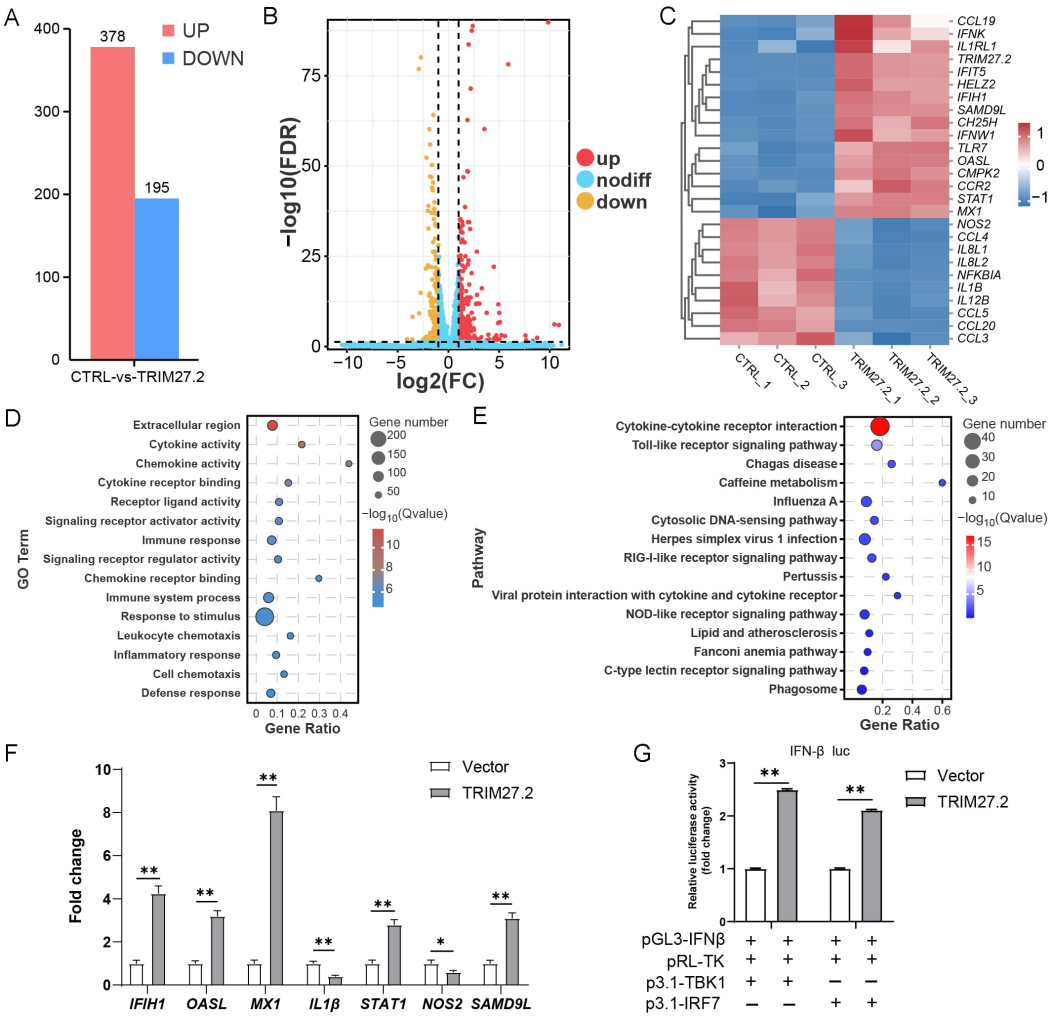


Figure 3. TRIM27.2 enhances antiviral gene expression in HD11 cells and IFN-β promoter activity in DF-1 cells. (**A**) Numbers of differentially expressed genes between the TRIM27.2 overexpression and control groups, including 378 upregulated and 195 downregulated genes. (**B**) Volcano plot of the differentially expressed genes. (**C**) Clustered heatmap of immune-related genes. Red and blue indicate relatively high and low expression levels, respectively. (**D**) Gene Ontology enrichment analysis of the differentially expressed genes. (**E**) Kyoto Encyclopedia of Genes and Genomes pathway enrichment analysis of the differentially expressed genes. (**F**) qRT-PCR validation of representative differentially expressed genes. (**G**) Dual-luciferase reporter assay in DF-1 cells showing the effect of TRIM27.2 on TBK1- or IRF7-induced IFN-β promoter activity. Data are presented as the mean ± SD ($n = 3$). * $p < 0.05$; ** $p < 0.01$.

3.4. Effects of Multiple Functional Domains of TRIM27.2 on MDA5–IFN-β Signaling

TRIM27.2 contains four predicted domains: RING, B-box, coiled-coil, and SPRY. To examine their contributions to immune-related gene expression, we constructed three

deletion mutants: TRIM27.2-delR, lacking the RING domain; TRIM27.2-delB&C, lacking the B-box and coiled-coil domains; and TRIM27.2-delS, lacking the SPRY domain (Figure 4A). Expression of full-length TRIM27.2 and all three mutants was confirmed by Western blotting (Figure 4B). qRT-PCR analysis showed that full-length TRIM27.2 increased the mRNA levels of MDA5, IFN-β, TBK1, and IRF7 compared with the empty-vector control (Figure 4C). All three deletion mutants showed smaller increases in MDA5 expression than full-length TRIM27.2. They also showed smaller increases in IFN-β expression, with TRIM27.2-delS producing the lowest IFN-β level among the mutants. In contrast, TBK1 and IRF7 expression varied less between full-length TRIM27.2 and the mutants (Figure 4C). These results suggest that multiple domains contribute to the effects of TRIM27.2 on MDA5 and IFN-β mRNA expression, although differences in mutant protein abundance should be considered when comparing their effects.

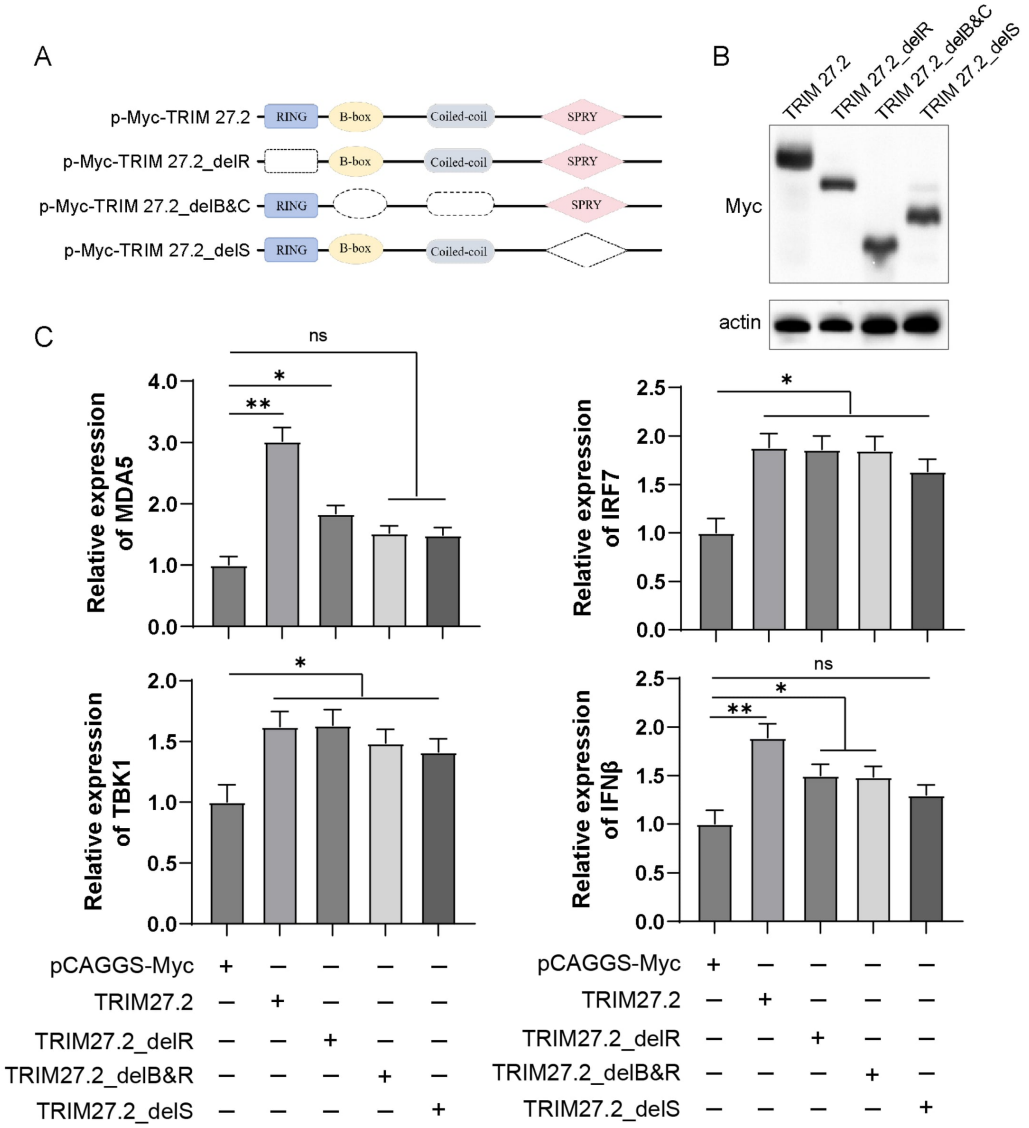


Figure 4. Effects of multiple functional domains of TRIM27.2 on MDA5–IFN-β signaling. (**A**) Schematic representation of full-length TRIM27.2 and its deletion mutants: delR, lacking the RING domain; delB&C, lacking the B-box and coiled-coil domains; and delS, lacking the SPRY domain. (**B**) Western blot analysis confirming the expression of full-length TRIM27.2 and its deletion mutants in HD11 cells. (**C**) Relative mRNA expression levels of MDA5, IFN-β, TBK1, and IRF7 following transfection with full-length TRIM27.2 or the indicated deletion mutants. Data are presented as the mean ± SD from three independent biological replicates. * $p < 0.05$; ** $p < 0.01$; ns, not significant.

3.5. Identification of USP19 as a Candidate TRIM27.2-Interacting Protein

To identify proteins that interact with TRIM27.2, Myc-TRIM27.2 was overexpressed in HD11 cells and immunoprecipitated using an anti-Myc antibody, with isotype IgG used as a negative control. Coomassie Brilliant Blue staining showed several protein bands enriched in the anti-Myc immunoprecipitation group compared with the input and IgG control groups (Figure 5A). The selected bands were analyzed by liquid chromatography–tandem mass spectrometry. Fifteen candidate TRIM27.2-interacting proteins were selected for presentation: SEC13, ATXN2, USP19, PHIP, GCLM, IGF2BP1, NCBP3, D2HGDH, DNAJC10, BF2, GTSE1, EPSTI1, LSM14A, RPF1, and ATP12A (Figure 5B). USP19, a deubiquitinating enzyme, was identified with 16 unique peptides, the highest number among the 15 candidates presented, and was therefore selected for further study.

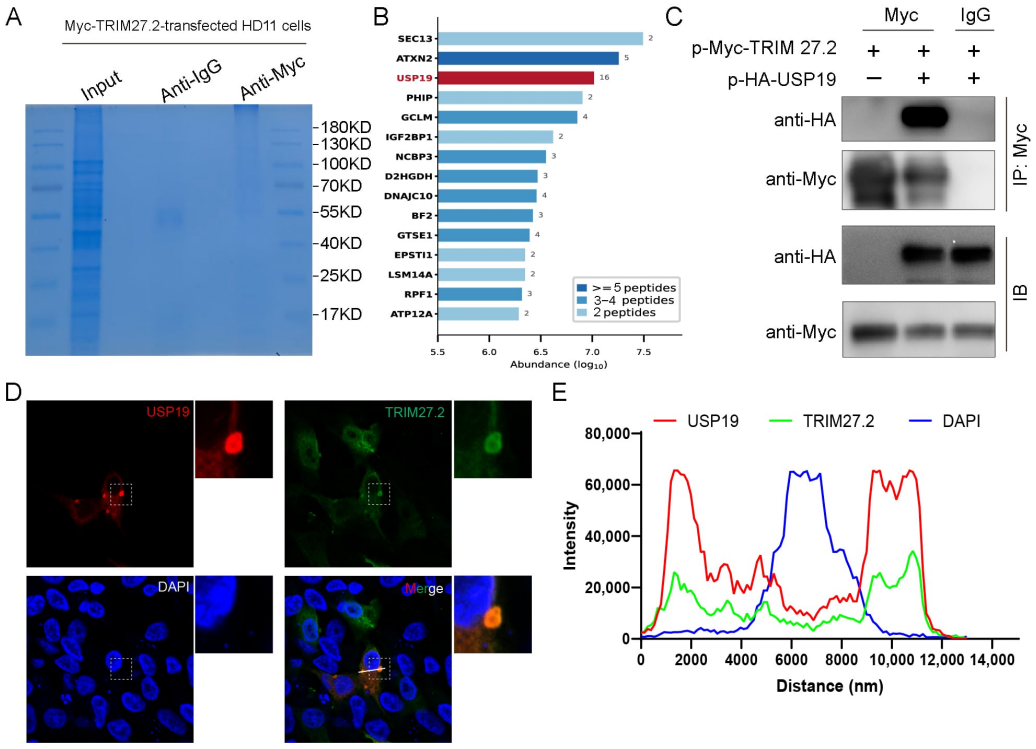


Figure 5. Identification of USP19 as a candidate TRIM27.2-interacting protein. (**A**) Gel staining of proteins immunoprecipitated from Myc-TRIM27.2-expressing HD11 cells using an anti-Myc antibody. Input, anti-IgG, and anti-Myc samples are shown. (**B**) Candidate TRIM27.2-interacting proteins identified by mass spectrometry and their relative abundance, expressed as $\log_{10}$ values. USP19 is highlighted in red, and the numbers to the right of the bars indicate the numbers of unique peptides identified. (**C**) Co-immunoprecipitation analysis of the interaction between TRIM27.2 and USP19. HA-USP19 was detected after immunoprecipitation with an anti-Myc antibody, and IgG was used as a negative control. (**D**) Immunofluorescence analysis of the colocalization of USP19 and TRIM27.2. USP19 is shown in red, TRIM27.2 in green, and nuclei stained with DAPI in blue. (**E**) Fluorescence intensity profiles of USP19 and TRIM27.2 along the indicated line.

The interaction between TRIM27.2 and USP19 was examined by co-immunoprecipitation after Myc-TRIM27.2 and HA-USP19 were coexpressed in HD11 cells. HA-USP19 was detected after immunoprecipitation with the anti-Myc antibody but was not detected in the IgG control (Figure 5C), supporting an association between the two proteins under overexpression conditions. Immunofluorescence analysis showed overlapping cytoplasmic signals for USP19 (red) and TRIM27.2 (green), producing a clear yellow signal in the merged image (Figure 5D). Their fluorescence intensity profiles also showed similar spatial distributions

along the selected line (Figure 5E). These results support the cytoplasmic colocalization of TRIM27.2 and USP19.

3.6. TRIM27.2 Promotes K48-Linked Polyubiquitination of USP19

Because TRIM27.2 contains a RING domain with potential E3 ubiquitin ligase activity and USP19 is a deubiquitinating enzyme, we examined whether their interaction affected USP19 ubiquitination. Under TRIM27.2 and USP19 coexpression conditions, treatment with the proteasome inhibitor MG132 increased the accumulation of both proteins, whereas chloroquine treatment had a limited effect (Figure 6A). These findings indicate that the turnover of TRIM27.2 and USP19 is sensitive to proteasome inhibition.

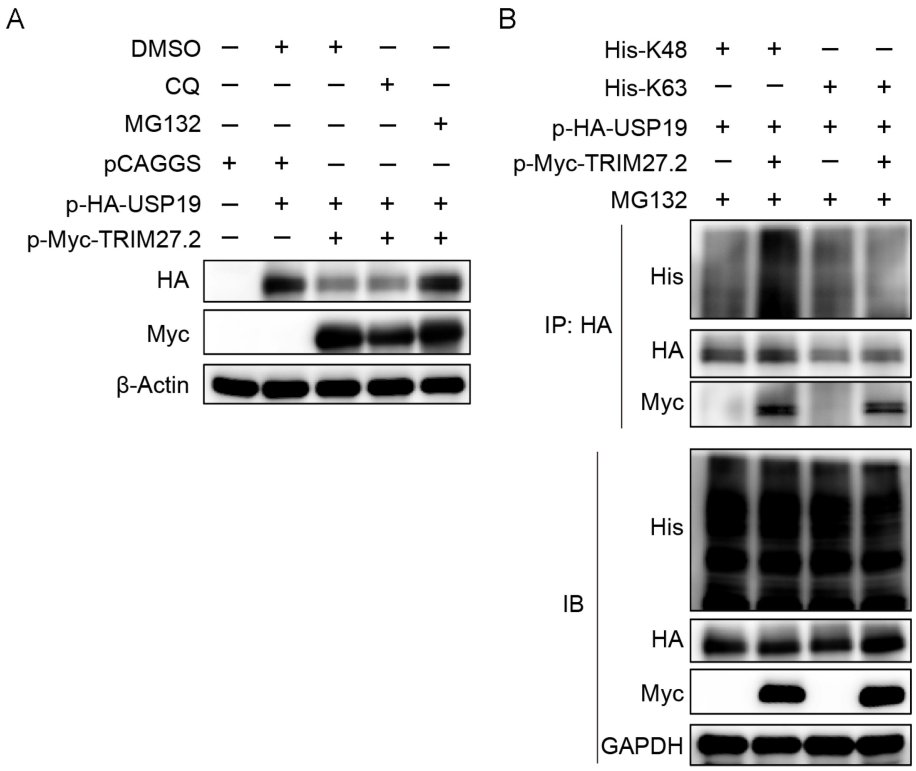


Figure 6. TRIM27.2 promotes K48-linked ubiquitination of USP19. (**A**) Effects of treatment with DMSO, chloroquine (CQ; 50 μmol/L), or MG132 (20 μmol/L) on the protein levels of HA-USP19 and Myc-TRIM27.2. β-Actin was used as the loading control. (**B**) Analysis of USP19 ubiquitination following cotransfection with His-tagged K48 or K63 ubiquitin constructs. Cells were treated with MG132, and HA-USP19 was immunoprecipitated using an anti-HA antibody (IP: HA). Ubiquitinated USP19 was detected using an anti-His antibody (IB: His). HA-USP19, Myc-TRIM27.2, and GAPDH were detected as expression and loading controls.

USP19 ubiquitination was subsequently examined by cotransfecting His-tagged K48 or K63 ubiquitin constructs, followed by immunoprecipitation with an anti-HA antibody. In the presence of MG132, TRIM27.2 coexpression increased the K48-linked ubiquitination signal of USP19. A K63-linked ubiquitination signal was also detected (Figure 6B). These results show that TRIM27.2 overexpression promotes K48-linked ubiquitination of USP19. Together with the reduction in USP19 protein abundance and its recovery following MG132 treatment, the results suggest that TRIM27.2 promotes the proteasomal degradation of USP19.

3.7. USP19 Knockdown Enhances the TRIM27.2-Mediated Antiviral Response

To determine the role of USP19 in ALV-J infection and its relationship with TRIM27.2, three siRNAs targeting chicken USP19 were evaluated. All three siRNAs significantly re-

duced USP19 mRNA expression ($p < 0.01$; Figure 7A). siUSP19_2 and siUSP19_3 showed the highest knockdown efficiencies and were selected for subsequent experiments. Following ALV-J infection, USP19 knockdown significantly reduced Env protein expression ($p < 0.01$; Figure 7B) and viral titers in the culture supernatant ($p < 0.05$; Figure 7D). In contrast, HA-USP19 overexpression significantly increased Env protein expression ($p < 0.01$; Figure 7C) and viral titers ($p < 0.05$; Figure 7E). These results indicate that USP19 promotes ALV-J replication. USP19 knockdown in TRIM27.2-overexpressing cells further increased MDA5 and IFN-β expression (Figure 7F). TRIM27.2 overexpression alone did not significantly increase MX1 expression, whereas USP19 knockdown combined with TRIM27.2 overexpression significantly increased MX1 expression ($p < 0.01$; Figure 7F). Following ALV-J infection, USP19 knockdown also enhanced TRIM27.2-mediated increases in IFN-β and MX1 expression and further reduced ALV-J RNA levels ($p < 0.05$; Figure 7G).

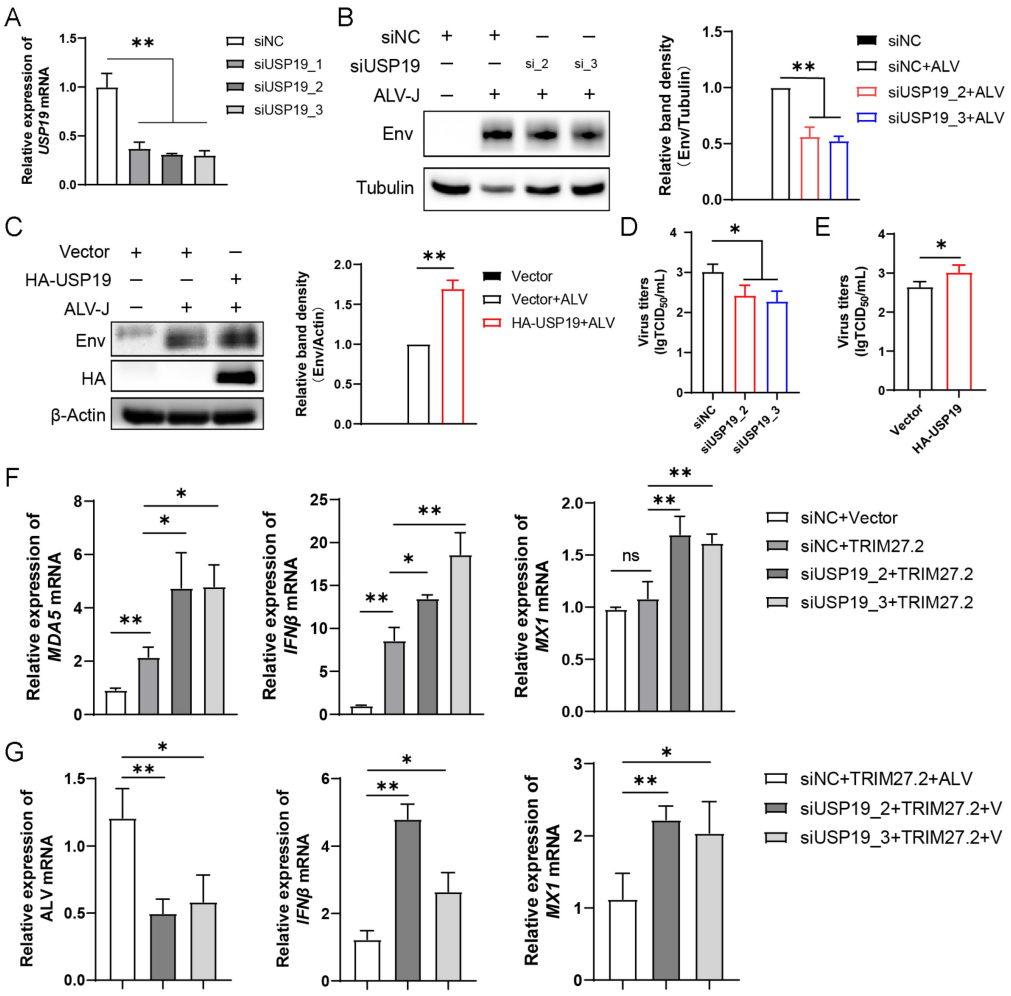


Figure 7. USP19 promotes ALV-J replication and inhibits TRIM27.2-mediated antiviral signaling. (**A**) Knockdown efficiencies of three USP19-specific siRNAs in HD11 cells. (**B**) Effect of USP19 knockdown on ALV-J Env protein expression (**left**) and densitometric analysis of the protein bands (**right**). (**C**) Effect of HA-USP19 overexpression on ALV-J Env protein expression (**left**) and densitometric analysis of the protein bands (**right**). (**D**) Effect of USP19 knockdown on viral titers. (**E**) Effect of USP19 overexpression on viral titers. (**F**) Effects of USP19 knockdown on TRIM27.2-induced expression of MDA5, IFN-β, and MX1. (**G**) Effects of USP19 knockdown on ALV-J RNA levels and TRIM27.2-mediated expression of IFN-β and MX1 following ALV-J infection. Data are presented as the mean ± SD from three independent biological replicates. * $p < 0.05$; ** $p < 0.01$; ns, not significant.

4. Discussion

ALV-J infection significantly altered the expression of several TRIM genes in the chicken MHC-B region, with clear differences in the direction, magnitude, and timing of their responses. TRIM41 showed the greatest increase, reaching approximately 30-fold the baseline level at 48 h post-infection. TRIM27.1, TRIM7.2, and TRIM39.1 were also significantly upregulated during the late stage of infection, whereas TRIM27.2 and TRIM39.2 were downregulated during the early stage. These differences suggest that the genes may be regulated differently during infection, but their expression patterns alone do not establish their functions. We focused on TRIM27.2 because its expression changed after infection and its role in chicken antiviral immunity had not been characterized. In particular, the early decrease in TRIM27.2 expression does not establish whether ALV-J actively suppresses this gene or whether the decrease favors viral replication. The mechanisms underlying this change and the roles of the other responsive TRIM genes remain to be determined.

Immunofluorescence analysis showed that exogenously expressed TRIM27.2 was distributed in both the cytoplasm and nucleus of HD11 cells (Figure 2A). When coexpressed with USP19, the nuclear fluorescence signal of TRIM27.2 decreased, and TRIM27.2 predominantly colocalized with USP19 in the cytoplasm (Figure 5D). These observations suggest that USP19 coexpression may be associated with changes in the subcellular distribution of TRIM27.2, although the underlying mechanism remains unclear. Functionally, TRIM27.2 overexpression reduced ALV-J RNA levels, infectious viral titers, and Env protein expression, indicating that TRIM27.2 inhibits ALV-J replication. Previous studies have shown that several chicken TRIM proteins possess antiviral activity. For example, chicken TRIM25 enhanced the MDA5-mediated type I interferon response and inhibited ALV-A replication [12], whereas increased TRIM45 expression inhibited ALV-J replication [21]. Together with these studies, our results suggest that TRIM27.2 restricts ALV-J replication by enhancing host antiviral responses. Because endogenous TRIM27.2 expression was low in HD11 cells, siRNA treatment did not achieve stable and sufficient knockdown. Its endogenous antiviral function therefore remains to be confirmed using a loss-of-function model. Future studies using CRISPR/Cas9-mediated TRIM27.2 knockout followed by gene complementation would help define the role of endogenous TRIM27.2 in ALV-J replication and MDA5–IFN-β signaling.

Transcriptome analysis showed that TRIM27.2 overexpression markedly altered the expression of immune-related genes in HD11 cells. Several interferon-stimulated genes (ISGs), including OASL, MX1, IFIT5, STAT1, SAMD9L, CH25H, and CMPK2, were upregulated, indicating that TRIM27.2 enhances the cellular antiviral transcriptional response. This finding was consistent with the reduced ALV-J replication and Env protein expression observed following TRIM27.2 overexpression. In contrast, several inflammation- and chemotaxis-related genes, including IL-1β, NOS2, IL-8L2, CCL3, CCL4, and CCL20, were downregulated. TRIM27.2 may therefore enhance antiviral responses while suppressing parts of the inflammatory transcriptional response. Chickens lack functional RIG-I; therefore, MDA5 plays an important role in recognizing cytoplasmic viral RNA and initiating antiviral immunity in chicken cells [11,22]. In this study, TRIM27.2 overexpression increased the expression of MDA5, TBK1, IRF7, and IFN-β, enhanced TBK1- or IRF7-induced IFN-β promoter activity, and promoted the expression of multiple downstream ISGs. A recent study showed that ALV-J induces miR-155 expression and suppresses type I interferon responses by targeting TRAF3 and STAT1, thereby facilitating viral replication [23]. This finding further highlights the importance of type I interferon responses in controlling ALV-J infection. Our results indicate that TRIM27.2 enhances MDA5–IFN-β-related antiviral signaling and its downstream transcriptional response. Transcriptome analysis also showed that TRIM27.2 reduced the expression of several inflammation- and chemotaxis-related

genes. Thus, TRIM27.2 may regulate both antiviral signaling and inflammation-related transcription. The biological effects of TRIM27.2 on inflammation and their relationship with its antiviral activity require further investigation.

Domain-deletion experiments showed that multiple functional domains of TRIM27.2 contribute to its regulation of MDA5 and IFN-β expression. Deletion of the RING domain attenuated this stimulatory activity. Because the RING domain commonly confers E3 ubiquitin ligase activity on TRIM proteins, its associated E3 activity may contribute to TRIM27.2-mediated enhancement of MDA5–IFN-β signaling. Together with the increased K48-linked ubiquitination and reduced protein abundance of USP19 following TRIM27.2 overexpression, these findings support a model in which TRIM27.2 regulates USP19 stability through ubiquitination and thereby enhances antiviral signaling. TRIM27-related proteins show different immunoregulatory functions among species. Mammalian TRIM27 promotes K48-linked ubiquitination and proteasomal degradation of TBK1, thereby inhibiting type I interferon production [15]. USP7 further enhances this inhibitory effect by stabilizing TRIM27 [16]. In contrast, duck TRIM27-L enhances MAVS signaling and promotes IFN-β and MX1 expression [17]. However, duck TRIM27-L is absent in chickens and turkeys and should not be considered functionally identical to the chicken MHC-B-linked TRIM27.2 examined in this study. Here, chicken TRIM27.2 promoted antiviral gene expression and restricted ALV-J replication. Its activity therefore differs from that of mammalian TRIM27 but shows some similarity to that of duck TRIM27-L. These findings suggest that the immune functions of TRIM27-related proteins are influenced by species differences, paralogous relationships, protein structure, and cellular context.

IP-MS identified USP19 as a candidate TRIM27.2-interacting protein. Their interaction was further confirmed by co-immunoprecipitation, while immunofluorescence analysis showed that TRIM27.2 and USP19 predominantly colocalized in the cytoplasm. TRIM27.2 contains a RING domain associated with E3 ubiquitin ligase activity, whereas USP19 is a deubiquitinating enzyme. Their interaction therefore suggests that they may jointly regulate the ubiquitination of proteins involved in antiviral signaling. Previous studies have shown that USP19 regulates autophagy and type I interferon responses by deubiquitinating Beclin-1, TRAF3, and MAVS [18–20]. In this study, TRIM27.2 overexpression increased K48-linked ubiquitination of USP19 and reduced its protein abundance, whereas the proteasome inhibitor MG132 partially restored USP19 accumulation. These results are consistent with TRIM27.2-associated K48-linked ubiquitination and proteasomal turnover of USP19, but do not directly demonstrate that TRIM27.2 ubiquitinates USP19 through its RING-associated E3 ligase activity.

Functional experiments further showed that USP19 plays a proviral role during ALV-J infection. USP19 knockdown reduced ALV-J Env protein expression and viral titers and further enhanced TRIM27.2-mediated expression of MDA5, IFN-β, and MX1. Conversely, USP19 overexpression promoted ALV-J replication. Previous studies in mammals have shown that USP19 negatively regulates type I interferon signaling [18–20], consistent with the enhanced antiviral response observed following USP19 knockdown in this study. Together with the increased K48-linked ubiquitination and reduced protein abundance of USP19, these results are consistent with a TRIM27.2–USP19–MDA5/IFN-β model in which TRIM27.2 promotes the ubiquitination and proteasomal degradation of USP19, and in which this contributes to the enhanced interferon-related transcription. Whether the enhancement of MDA5–IFN-β signaling is the means by which TRIM27.2 restricts ALV-J remains to be established directly. It should be emphasized that the conclusions of the present study are derived from gain-of-function experiments. Overexpression of TRIM27.2 was used because endogenous TRIM27.2 expression in HD11 cells was too low for reliable knockdown. The antiviral activity of TRIM27.2 therefore demonstrates an effect under the conditions tested,

and does not by itself establish the physiological contribution of endogenous TRIM27.2 to resistance to ALV-J.

Several limitations of the present study should be acknowledged. First, all functional experiments relied on overexpression of TRIM27.2 in a cell line; the physiological contribution of endogenous TRIM27.2 to resistance to ALV-J remains to be established using loss-of-function models. Second, the domain-deletion experiment measures transcriptional responses and does not directly demonstrate that the RING domain mediates the ubiquitination of USP19, and differences in the steady-state abundance of the deletion mutants limit the extent to which that experiment can be interpreted. Third, although the poly(I:C) stimulation experiment indicates that the TRIM27.2–USP19 axis influences interferon-related transcription when the MDA5 pathway is activated directly, strict MDA5 dependency has not been demonstrated and would require loss-of-function manipulation of MDA5 itself. Fourth, cell viability was confirmed to be comparable between the transfection groups used in the viral replication experiments, but the number of viable cells was not enumerated in every condition, so differences in viable cell number cannot be completely excluded as a contributor to the observed differences in viral titer. Finally, the co-immunoprecipitation and colocalization data establish association rather than direct binding, and the proposed redistribution of TRIM27.2 upon USP19 co-expression is based on spatial overlap only.

Host immune regulators, including protein-coding genes and regulatory RNAs, represent potential molecular targets for improving disease resistance in poultry [24]. The TRIM27.2–USP19–MDA5/IFN-β axis identified in this study expands the chicken antiviral immune network and provides candidate host factors for investigating resistance to ALV-J. In vivo infection studies, gene-knockout models, and genetic variation analyses in different chicken populations are needed to evaluate the potential value of TRIM27.2 and USP19 in disease-resistant breeding.

5. Conclusions

In conclusion, overexpression of chicken MHC-B-linked TRIM27.2 enhances MDA5–IFN-β-related antiviral transcription and restricts ALV-J replication under the tested cell-culture conditions. TRIM27.2 upregulates multiple ISGs while reducing the expression of several inflammation- and chemotaxis-related genes. Multiple functional domains contribute to its immunoregulatory activity, although the specific contribution of RING-dependent E3 activity remains to be established. Furthermore, USP19 was identified as a TRIM27.2-interacting protein, and TRIM27.2 overexpression was associated with increased K48-linked ubiquitination and proteasome-sensitive reduction in USP19. These findings support a proposed TRIM27.2–USP19–interferon-related regulatory model; whether this mechanism operates endogenously and is required for restriction of ALV-J remains to be tested.

Supplementary Materials: The following supporting information can be downloaded at https://www.mdpi.com/article/10.3390/ani16233793/s1. Figure S1. Principal component analysis (PCA) of RNA-seq data from CTRL and TRIM27.2-overexpressing HD11 cells. Table S1. Sequences of siRNAs targeting chicken USP19 and negative control (NC). Table S2. Primer sequences used in this study. Table S3. Proteins identified by LC–MS/MS analysis of TRIM27.2 immunoprecipitates. Table S4. Principal component analysis (PCA) of RNA-seq samples from the CTRL and TRIM27.2-overexpressing groups.

Author Contributions: Conceptualization, S.C. and G.C.; methodology, S.C. and Q.C.; software, Y.B.; validation, Q.C., Q.W. and N.Y.; formal analysis, J.W.; investigation, Q.C., Q.W. and N.Y.; resources, G.C.; data curation, J.W. and Y.B.; writing—original draft preparation, S.C. and Q.C.; writing—review and editing, Y.B. and G.C.; visualization, Q.C.; supervision, Y.B.; project administration, Y.B.; funding acquisition, S.C., Y.B. and G.C. All authors have read and agreed to the published version of themanuscript.

Funding: This study was supported by the National Natural Science Foundation of China (32272921), the Biological Breeding-National Science and Technology Major Project (2023ZD0405301), the China National Broiler Industry Technology System (Grant No. CARS-40).

Institutional Review Board Statement: Not applicable. Ethical review and approval were waived for this study, as all experiments were conducted in vitro with established cell lines, and no live animals or human samples were used.

Informed Consent Statement: Not applicable.

Data Availability Statement: All data supporting the findings of this study are contained within the article and its Supplementary Materials. The raw sequencing data generated in this study are publicly available in the Genome Sequence Archive (GSA) under accession number CRA052853 at https://ngdc.cncb.ac.cn/gsa/browse/CRA052853 (accessed on 2 November 2026).

Conflicts of Interest: The authors declare no conflicts of interest.

Abbreviations

The following abbreviations are used in this manuscript:

TRIM	Tripartite motif-containing protein
ALV-J	Avian leukosis virus subgroup J
ALV-A	Avian leukosis virus subgroup A
MHC	Major histocompatibility complex
MHC-B	Chicken major histocompatibility complex B locus
MDA5	Melanoma differentiation-associated protein 5
RIG-I	Retinoic acid-inducible gene I
IFN-β	Interferon beta
ISGs	Interferon-stimulated genes
TBK1	TANK-binding kinase 1
IRF7	Interferon regulatory factor 7
FDR	False discovery rate
$TCID_{50}$	50% tissue culture infectious dose
IP-MS	Immunoprecipitation–mass spectrometry

References

1. Payne, L.N.; Brown, S.R.; Bumstead, N.; Howes, K.; Frazier, J.A.; Thouless, M.E. A novel subgroup of exogenous avian leukosis virus in chickens. *J. Gen. Virol.* **1991**, *72*, 801–807. [CrossRef]
2. Fandino, S.; Gomez-Lucia, E.; Benitez, L.; Domenech, A. Avian Leukosis: Will We Be Able to Get Rid of It? *Animals* **2023**, *13*, 2358. [CrossRef]
3. Gao, Y.L.; Qin, L.T.; Pan, W.; Wang, Y.Q.; Le Qi, X.; Gao, H.L.; Wang, X.M. Avian leukosis virus subgroup J in layer chickens, China. *Emerg. Infect. Dis.* **2010**, *16*, 1637–1638. [CrossRef]
4. Liu, X.; Lan, X. Research Progress on Pathogenesis and Prevention of Avian Leukosis Virus J Subgroup (ALV-J). *Vet. Sci.* **2026**, *13*, 152. [CrossRef]
5. Feng, M.; Dai, M.; Xie, T.; Li, Z.; Shi, M.; Zhang, X. Innate Immune Responses in ALV-J Infected Chicks and Chickens with Hemangioma In Vivo. *Front. Microbiol.* **2016**, *7*, 786. [CrossRef]
6. Ruby, T.; Bed'Hom, B.; Wittzell, H.; Morin, V.; Oudin, A.; Zoorob, R. Characterisation of a cluster of TRIM-B30.2 genes in the chicken MHC B locus. *Immunogenetics* **2005**, *57*, 116–128. [CrossRef]
7. Shiina, T.; Briles, W.E.; Goto, R.M.; Hosomichi, K.; Yanagiya, K.; Shimizu, S.; Inoko, H.; Miller, M.M. Extended gene map reveals tripartite motif, C-type lectin, and Ig superfamily type genes within a subregion of the chicken MHC-B affecting infectious disease. *J. Immunol.* **2007**, *178*, 7162–7172. [CrossRef]
8. Wang, J.; Wang, Q.; Li, X.; Cai, Q.; Bi, Y.; Xu, C.; Bai, H.; Gu, L.; Chang, G.; Chen, S. Emerging roles of TRIM in metabolic regulation. *Metabolism* **2026**, *174*, 156394. [CrossRef]
9. Li, L.; Feng, W.; Cheng, Z.; Yang, J.; Bi, J.; Wang, X.; Wang, G. TRIM62-mediated restriction of avian leukosis virus subgroup J replication is dependent on the SPRY domain. *Poult. Sci.* **2019**, *98*, 6019–6025. [CrossRef]
10. Karpala, A.J.; Stewart, C.; McKay, J.; Lowenthal, J.W.; Bean, A.G. Characterization of chicken Mda5 activity: Regulation of IFN-beta in the absence of RIG-I functionality. *J. Immunol.* **2011**, *186*, 5397–5405. [CrossRef]

11. Hayashi, T.; Watanabe, C.; Suzuki, Y.; Tanikawa, T.; Uchida, Y.; Saito, T. Chicken MDA5 senses short double-stranded RNA with implications for antiviral response against avian influenza viruses in chicken. *J. Innate Immun.* **2014**, *6*, 58–71. [CrossRef]
12. Zhou, J.R.; Liu, J.H.; Li, H.M.; Zhao, Y.; Cheng, Z.; Hou, Y.M.; Guo, H.J. Regulatory effects of chicken TRIM25 on the replication of ALV-A and the MDA5-mediated type I interferon response. *Vet. Res.* **2020**, *51*, 145. [CrossRef]
13. Yu, M.; Zhang, L.; Wang, Y.; Wang, S.; Liu, Y.; Liu, P.; Chen, Y.; Guo, R.; Meng, L.; Zhang, T.; et al. N6-methyladenosine modification of the subgroup J avian leukosis viral RNAs attenuates host innate immunity via MDA5 signaling. *PLoS Pathog.* **2025**, *21*, e1013064. [CrossRef]
14. Li, Z.; Luo, Q.; Xu, H.; Zheng, M.; Abdalla, B.A.; Feng, M.; Cai, B.; Zhang, X.; Nie, Q.; Zhang, X. MiR-34b-5p Suppresses Melanoma Differentiation-Associated Gene 5 (MDA5) Signaling Pathway to Promote Avian Leukosis Virus Subgroup J (ALV-J)-Infected Cells Proliferaction and ALV-J Replication. *Front. Cell Infect. Microbiol.* **2017**, *7*, 17. [CrossRef]
15. Zheng, Q.; Hou, J.; Zhou, Y.; Yang, Y.; Xie, B.; Cao, X. Siglec1 suppresses antiviral innate immune response by inducing TBK1 degradation via the ubiquitin ligase TRIM27. *Cell Res.* **2015**, *25*, 1121–1136. [CrossRef]
16. Cai, J.; Chen, H.Y.; Peng, S.J.; Meng, J.L.; Wang, Y.; Zhou, Y.; Qian, X.P.; Sun, X.Y.; Pang, X.W.; Zhang, Y.; et al. USP7-TRIM27 axis negatively modulates antiviral type I IFN signaling. *FASEB J.* **2018**, *32*, 5238–5249. [CrossRef]
17. Blaine, A.H.; Miranzo-Navarro, D.; Campbell, L.K.; Aldridge, J.R., Jr.; Webster, R.G.; Magor, K.E. Duck TRIM27-L enhances MAVS signaling and is absent in chickens and turkeys. *Mol. Immunol.* **2015**, *67*, 607–615. [CrossRef]
18. Jin, S.; Tian, S.; Chen, Y.; Zhang, C.; Xie, W.; Xia, X.; Cui, J.; Wang, R.F. USP19 modulates autophagy and antiviral immune responses by deubiquitinating Beclin-1. *EMBO J.* **2016**, *35*, 866–880. [CrossRef]
19. Gu, Z.; Shi, W.; Zhang, L.; Hu, Z.; Xu, C. USP19 suppresses cellular type I interferon signaling by targeting TRAF3 for deubiquitination. *Future Microbiol.* **2017**, *12*, 767–779. [CrossRef]
20. Weerawardhana, A.; Herath, T.U.B.; Gayan Chathuranga, W.A.; Kim, T.H.; Ekanayaka, P.; Chathuranga, K.; Kang, H.C.; Jung, J.U.; Lee, J.S. SIAH1 modulates antiviral immune responses by targeting deubiquitinase USP19. *J. Med. Virol.* **2024**, *96*, e29523. [CrossRef]
21. Wang, J.; Wang, Q.; Ping, Y.; Huang, X.; Yang, T.; Bi, Y.; Chang, G.; Chen, S. Identification and characterization of chicken TRIM45 and its role as a negative regulator of ALV-J replication in vitro. *Avian Pathol.* **2025**, *54*, 255–264. [CrossRef]
22. Magor, K.E. Evolution of RNA sensing receptors in birds. *Immunogenetics* **2022**, *74*, 149–165. [CrossRef]
23. Zhang, X.; Zhou, D.; Zhou, J.; Liu, X.; Ding, L.; Yan, T.; Shi, M.; He, S.; Cheng, Z. Avian leukosis virus subgroup J evades innate immunity by activating miR-155 to dually target TRAF3 and STAT1. *PLoS Pathog.* **2025**, *21*, e1013552. [CrossRef]
24. Wang, Q.; Wu, W.; Cai, Q.; Wang, J.; Gao, Q.; Iftikhar, M.; Bi, Y.; Bai, H.; Gu, L.; Chang, G.; et al. The Role of miRNAs in Chicken Immune Regulation and Prospects for Disease-Resistant Breeding. *Anim. Res. One Health* **2025**, *4*, 419–434. [CrossRef]

Disclaimer/Publisher's Note: The statements, opinions and data contained in all publications are solely those of the individual author(s) and contributor(s) and not of MDPI and/or the editor(s). MDPI and/or the editor(s) disclaim responsibility for any injury to people or property resulting from any ideas, methods, instructions or products referred to in the content.